INTERHEMISPHERIC DIFFERENCES IN CO_2 SUPERSATURATION AND CO_2 GAS DEPLETION IN MARS' POLAR WINTER ATMOSPHERE FROM MARS CLIMATE SOUNDER OBSERVATIONS.

A. Kleinböhl[1], D. M. Kass[1], S. Piqueux[1], P. O. Hayne[2], and K. Noguchi[3], [1]Jet Propulsion Laboratory, California Institute of Technology, Pasadena, CA, [2]Laboratory for Atmospheric and Space Physics, University of Colorado, Boulder, CO, [3]Nara Women's University, Nara, Japan. (Armin.Kleinboehl@jpl.nasa.gov)

Introduction: Temperatures in the martian lower atmosphere commonly reach the frost point of CO_2 in polar winter conditions [1,2]. Temperature retrievals using data from the Mars Climate Sounder (MCS) reveal that temperatures in the south winter polar region repeatedly drop several K below the frost point of CO_2. In contrast, temperatures in the north polar winter region tend to be very close to the CO_2 frost point. Temperatures below the CO_2 frost point indicate supersaturation of the atmosphere with respect ot CO_2. This can occur due to a lack of condensation nuclei, or due to condensation nuclei being very small, leading to large contact angles and low nucleation efficiencies [3]. Depressed temperatures in polar winter can be caused by the removal of CO_2 from the atmosphere through condensation, resulting in an atmosphere that is depleted in gaseous CO_2 and enhanced in non-condensables like N_2 and Ar. The reduced CO_2 mixing ratio reduces the condensation temperature and requires a colder atmospehre for a given degree of supersaturation. We evaluate differences in the temperature structure between the north and south polar winter atmospheres with respect to CO_2 supersaturation and CO_2 gas depletion.

MCS Instrument and Retrievals: The Mars Climate Sounder [6] is a passive infrared radiometer onboard Mars Reconnaissance Orbiter (MRO), which views the martian atmosphere in limb and on-planet geometries. It has five mid-infrared, three far infrared, and one broadband visible/near-infrared channels. Each spectral channel uses a linear detector array consisting of 21 elements, which provides -10 to 90 km altitude coverage with 5 km vertical sampling when pointed at the Mars limb.

Profile retrievals from MCS radiance measurements use a modified Chahine method together with a Curtis-Godson approximation in the radiative transfer [7] and employ a single-scattering approximation to account for scattering in the limb radiative transfer [8].

This study is enabled by retrievals with a 2D radiative transfer scheme for orbital limb emission measurements in the infrared [9], which describes horizontal gradients using consecutive limb measurements by MCS in the forward direction along the orbit track. The lines-of-sight of these limb views overlap significantly, allowing the characterization of horizontal gradients

for a particular measurement through information from its neighboring measurements.

Retrievals of temperature use the MCS mid-infrared channels A1, A2, and A3 that cover frequencies within the 15 μm gaseous absorption band of CO_2. Aerosol extinction retrievals are based on limb measurements in channel A4, centered on a water ice absorption feature at 12 μm, and channel A5, covering an absorption feature of Mars dust around 22 μm. We note that channel A5 is also sensitive to CO_2 ice occurring in the lower atmosphere of the winter polar regions. Atmospheric CO_2 ice in these regions is characterized by large particle sizes, leading to an extinction spectrum that is comparatively flat over a large range of infrared wavelengths [10]. For this analysis dust spectroscopic parameters are used [8]. Comparisons indicate that the use of dust vs. CO_2 ice spectroscopic parameters has virtually no influence on the result of the temperature retrieval.

Results: Figure 1 shows examples of profile retrievals of temperature in the core of the southern polar vortex at L_s=130°-135°. Temperatures at pressures over ~20 Pa (below ~20 km altitude) are consistently below the CO_2 frost point calculated for a 95% mixing ratio of CO_2 (black dashed line). On average the temperature profiles in the lower atmosphere parallel the frost point with a separation of about 4 K.

Figure 2 shows the temperature development in the south polar region over the course of the winter. The temperature rapidly drops below the CO_2 frost point. Aerosol measurements suggest that CO_2 ice forms al-
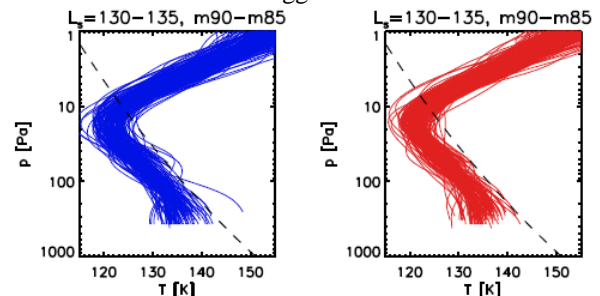

Figure 1: Retrieved temperature profiles from MCS observations in the south polar region on the nighttime (left) and daytime (right) parts of the MRO orbit between 90°S and 85°S in Mars Year 33. The dashed line indicates the CO_2 frost point.
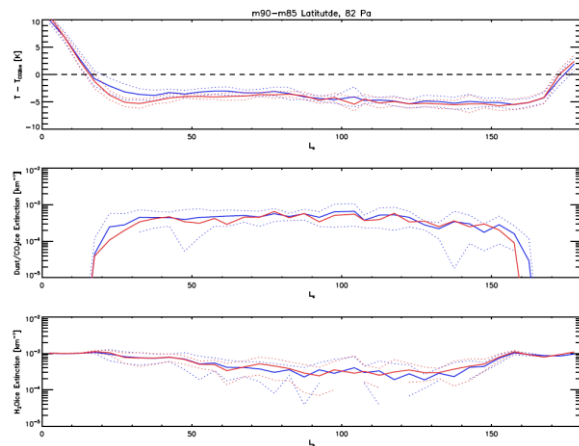
Figure 2: Averages of retrieved temperatures with respect the CO_2 frost point (top), carbon dioxide ice extinction (retrieved as dust extinction, center) and water ice extinction (bottom) vs. L_s from MCS measurements at a pressure level of 82 Pa (~12 km altitude) between 90°S and 85°S in Mars Year 33. Colors indicate measurements on the nightside (blue) and dayside (red) parts of the orbit.

Figure 3: As in Figure 2 but between 85°N and 90°N in Mars Year 32.

most immediately at the beginning of the winter, likely aided by water ice as condensation nuclei, which is present at extinction levels around 10^{-3} km^{-1}. The temperature depression below the frost point is about 4 K at the beginning of the winter. It is unlikely that widespread depletion of CO_2 has taken place already at the beginning of the winter, suggesting that the temperature effect is caused by supersaturation. The observed temperature depression corresponds to a supersaturations in the order of 1.8. This is somewhat higher than suggested by model calculations and laboratory measurements [11,12] but in family with reanalyses of radio science temperature measurements [13].

Towards the end of the winter the temperature dips up to ~5 K below the frost point. After L_s=160° only little CO_2 ice opacity is observed anymore (Figure 2). We assume that part of this temperature depression is caused by the depletion of CO_2 gas due to CO_2 frost formation on the surface [14] and CO_2 ice formation in the atmosphere followed by sedimentation. It is unlikely that the temperature depression is solely caused by this effect as this would suggest unrealistically low CO_2 mixing ratios in comparison to previous measurements [4,5]. Assuming a supersaturation at the same levels as observed in the beginning of the winter, the observed additional temperature depression can be explained by CO_2 depletion corresponding to about a six-fold enhancement in N_2 and Ar, in family with the enhancement derived from γ-ray spectroscopy [4,5].

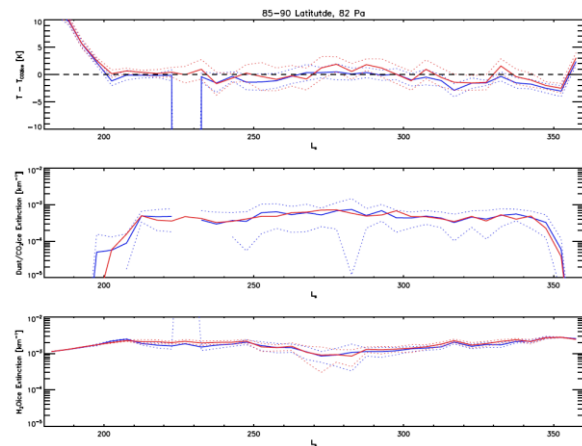Figure 3 shows the same information as Figure 2 but for the north polar winter in Mars Year 33. In con-

trast to the south polar region, temperatures in the north stay very close to the CO_2 frost point, and only dip below by 1-2 K towards the end of the winter. This indicates that neither widespread supersaturation nor CO_2 depletion of significant magnitude were present, suggesting that the polar vortex in the north is less isolated than in the south. Water ice extinctions in the north polar region are with 2-$3 \bullet 10^{-3}$ km^{-1} somewhat higher than in the south. The higher availability of water ice particles as condensation nuclei likely contributes to the lack of supersaturation in the north polar region. In terms of CO_2 depletion, the observed behavior is consistent with results from γ-ray spectroscopy, which finds little enhancement of non-condensables at northern high latitudes [4,5].

References: [1] McCleese, D. J. et al. (2008) NGeo, 1, 745-749. [2] McCleese, D. J. et al. (2010) JGR, 115, E12016. [3] Wood, S. E., (1999), PhD thesis, UCLA. [4] Sprague, A. L. et al. (2004) Science, 306, 1364-1367. [5] Sprague, A. L. et al. (2012) JGR, 117, E04005. [6] McCleese, D. J. et al. (2007) JGR, 112, E05S06. [7] Kleinböhl, A. et al. (2009) JGR, 114, E10006. [8] Kleinböhl, A. et al. (2011) JQSRT, 112, 1568-1580. [9] Kleinböhl, A. et al. (2017) JQSRT, 187, 511-522. [10] Hayne, P. O. et al. (2012) JGR, 117, E08014. [11] Määttänen, A. et al. (2005) JGR, 110, E02002. [12] Glandorf, D. L. et al. (2002) Icarus, 160, 66–72. [13] Noguchi, K. et al. (2014) JGR, 119, 2510–2521. [14] Piqueux, S. et al. (2019) this conference.